Efficient Learning Control through Zonotopic Set Membership Estimation and Scenario MPC*

Qian Shi[1], Andres Cordoba-Pacheco[1], and Fredy Ruiz[1]

***Abstract*— Model Predictive Control (MPC) is widely used in control systems due to its proficiency in managing input and state constraints while optimizing controller performance. Nevertheless, applying MPC to systems with uncertain disturbances and unknown dynamics presents formidable challenges. To handle this issue, we propose a learning scenario-MPC approach. An auto-regressive model with exogenous input is iteratively identified, and its parameters are randomly sampled from an updated zonotopic feasible parameter set. The MPC framework is then implemented using the updated auto-regressive model set as dynamic constraints, with a mean cost function, computed across the predefined set of sampled scenarios. This approach leads to a low complexity adaptive control strategy with probabilistic guarantees on constraint satisfaction. The effectiveness of the proposed method is validated on a vehicle path following problem, with unknown vehicle parameters and varying curvatures, where it is shown that the strategy is able to learn the system dynamics from closed-loop data while properly tracking the target path.**

I. Introduction

Some of the most challenging control problems are characterized by nonlinear dynamics with inherent uncertainties and safety-critical constraints. Model Predictive Control (MPC) can provide high-performance control for complex systems while satisfying general state and input constraints [1], [2]. Nevertheless, its performance is influenced by the accuracy of the prediction model. Under model uncertainty and disturbances, the desired closed-loop properties, including stability, performance, and constraint satisfaction, are generally not guaranteed.

Over the past few decades, Robust Model Predictive Control (RMPC) has had significant attention with the aim of guaranteeing stability and constraint satisfaction under model uncertainties and external disturbances [3], [4].RMPC methodologies typically achieve this by predicting a tube or funnel over the prediction horizon that encapsulates all potential uncertain state trajectories. The literature presents diverse RMPC approaches, differing in terms of their conservatism and computational complexity [5]–[7]. Traditionally, RMPC adopts min-max formulations, optimizing control actions for the worst-case scenarios of model uncertainty or disturbance realizations [8], [9]. However, satisfying constraints for all possible uncertainty values can be overly conservative. Moreover, the computational demands of RMPC methods do not scale well with increasing model and disturbance complexities, sometimes requiring ad hoc simplifications of the constraints.

When model uncertainties have a known probabilistic description, Stochastic Model Predictive Control (SMPC) can enforce state and input constraints as chance constraints [10], [11]. By allowing a small probability of constraint violation, SMPC reduces the conservatism of RMPC solutions, particularly in rare-event scenarios. It relaxes robust control by trading off constraint satisfaction against improved cost function performance (in terms of the cost function). A primary challenge in numerous SMPC approaches is solving chance-constrained finite-horizon optimal control problems (FHOCPs) at each sampling time step. These problems correspond to nonconvex stochastic programs, for which finding an exact solution is computationally intensive. To achieve a computationally tractable solution, various sample-based approximation methods have been proposed [12], [13].

Model mismatch often arises from inaccurate system knowledge and incorporating online model updates can enhance RMPC performance [14]. For linearly parameterized models with bounded disturbances, parameter sets can be efficiently updated using estimation techniques [15]. In particular, Set Membership estimation is a well-established approach for dealing with uncertainty in system identification and control [16]–[18].

Building upon the discussed methodologies, this work proposes a general yet tractable scenario-based adaptive framework for chance-constrained stochastic MPC with linear uncertain dynamics. The proposed method identifies the system using an AutoRegressive with eXogenous input (ARX) model, enabling a data-driven approach. The model parameters are iteratively updated through Set Membership estimation, while computational complexity is reduced by enforcing probabilistic constraint satisfaction through a scenario approach. To further enhance tractability, model uncertainty is represented using zonotopes, allowing an efficient update of the feasible model set and facilitating the sampling scheme for randomized optimization. This integration of adaptive learning and scenario-based stochastic MPC advances existing techniques by improving scalability, reducing conservatism, and enhancing computational efficiency in handling uncertainty.

II. Modeling and Uncertainty Representation

In this section we describe the model parametrization and the iterative identification procedure that is incorporated into the MPC strategy in Section III.

[1]Dipartimento di Elettronica, Informazione e Bioingegneria, Politecnico di Milano, Milan, Italy {qian.shi, andresfelipe.cordoba, fredy.ruiz}@polimi.it

*This research has been supported by the Italian Ministry of University and Research under grant "Learning-based Model Predictive Control by Exploration and Exploitation in Uncertain Environments" (PRIN PNRR 2022 fund, ID P2022EXP2W).

Consider an uncertain Linear Time-Invariant (LTI) system in discrete time. We denote the system input at time step t by $u(t)$ and output by $y(t)$. We assume that the dynamic relation between inputs and outputs can be described by an ARX model. Without loss of generality, the formulation is presented for Single Input-Single Output systems.

Consider an ARX model with known orders na and nb. The plant output $y(t)$ is given by:

$$y(t+1) = \sum_{i=1}^{n_a} a_i y(t-i+1) + \sum_{i=1}^{n_b} b_i u(t-i+1) + d(t) \quad (1)$$

where $d(t)$ denotes the contribution of disturbances and unknown dynamics to the output. The approximation error is embedded into $d(t)$.

Defining the regressor

$$\begin{aligned} z(t+1) \quad = \quad & [y(t), y(t-1), ..., y(t-na+1), \\ & u(t), u(t-1), ..., u(t-nb+1)], \end{aligned}$$

the ARX model can be expressed as:

$$y(t+1) = \theta^\top z(t+1) + d(t) \quad (2)$$

where $\theta = [a_1, a_2, ..., a_{n_a}, b_1, b_2, ..., b_{n_b}]^\top$ is the parameter vector that defines the system.

The measured output available for feedback control is corrupted by noise, as $\tilde{y}(t) = y(t) + v(t)$ where $v(t)$ is measurement noise.

Assumption 1: $d(t)$ and $v(t)$ are Unknown But Bounded (UBB) signals, such that for all t:

$$\begin{aligned} |d(t)| &\leq \epsilon_d \\ |v(t)| &\leq \epsilon_v \end{aligned} \quad (3)$$

where ϵ_d and ϵ_v are positive scalars.

Note that parameters θ in (1) remain to be identified. Given a set of input and output measurements, using an SM framework, the system parameters belong to the Feasible Systems Set (FSS), that is, the set of all model parameters θ compatible with available data and the assumed noise bounds. This approach is suitable for robust controller design in a subsequent step.

Given a sequence of samples $(\tilde{y}(t), z(t))$, the FSS for model (1) can be determined recursively as:

$$\begin{aligned} & FSS_{0,T} = \cap_{t=0}^{T} FSS(t) \\ & FSS(t) = \{\theta : |\tilde{y}(t) - \theta^\top z(t)| \leq \epsilon_d + \epsilon_v\} \\ & FSS(0) = FSS_0. \end{aligned} \quad (4)$$

where FSS_0 is the set of parameters defined by the a priori information about the system, and T is the terminal time step. This formulation differs from the standard SM formulation, where a batch of data is used to define $FSS_{0,T}$ in a single step.

Note that, provided that FSS_0 is a convex set, $FSS_{0,T}$ is also convex, considering that $FSS(t)$ is a strip. However, in practice, it is impossible to handle the FSS as measurement data increases. Instead, at each time instant t an approximated feasible system set $AFSS(t)$ ($AFSS(t) \supset FSS(t)$), constructed as an outer approximation of the FSS, is used to describe the parametric uncertainty:

$$AFSS(t) \supset AFSS_{0,t-1} \cap FSS(t). \quad (5)$$

In this work, zonotopes are selected to build the approximated sets due to their advantageous properties in handling uncertainty. Zonotopes offer high accuracy, compact representation, and low computational complexity compared to alternative uncertainty representation methods such as polytopes and ellipsoids [15], [19]. Zonotopes provide a flexible representation that allows an efficient update of sets over time and simple uncertainty sampling, key steps in stochastic adaptive control.

Zonotopes are affine mappings of unitary hypercubes and can be mathematically described as $M = p \bigoplus HB^m$, where $p \subset R^n$ is the center of M, $H \subset R^{n \times m}$ is the matrix of generators, $B = [-1, 1]$ is the unitary interval, and B^m means an m-order unitary box and '$\bigoplus$' denotes the Minkowski sum.

Assuming that $AFSS(t)$ is parametrized as a zonotope, the update of $AFSS(t)$ at each time step t can be performed efficiently by exploiting the following property:

Property 1: [15] Given the zonotope $Z = p \bigoplus HB^m \subset R^n$, the strip $S = \{x \subset |c^\top x - d| \leq \sigma\}$ and the vector $\lambda \subset R^n$, define $\hat{p}(\lambda) = p + \lambda(d - c^\top p)$,$\hat{H}(\lambda) = [(I - \lambda c^\top)H \ \sigma\lambda]$. Then, $Z \cap S \subset \hat{Z}(\lambda) = \hat{p}(\lambda) \bigoplus \hat{H}(\lambda) B^{m+1}$. λ is calculated as:

$$\lambda = \frac{-Ab}{b^\top b} = \frac{HH^\top c}{c^\top HH^\top c + \sigma^2}. \quad (6)$$

The complexity of algorithms that act on zonotopes strongly depends on their order (i.e. the number of generators and dimensions), which is increased by intersection and Minkowski sum operations. Thus, to keep computations efficient, zonotopes of high orders can be over-approximated as tight as possible by zonotopes of smaller order. In this research, the order of zonotopes is reduced by the principle component analysis method proposed in [20] and described in Algorithm 1, where Z_{red} denotes a zonotope with reduced order.

Algorithm 1 Order Reduction Algorithm for Zonotope

1: Input: Zonotope $Z = p \bigoplus HB^m$;
2: Output: Zonotope Z_{red};
3: $X = [H \quad -H]^\top$;
4: Covariance: $Co = X^\top X$;
5: Decomposition: $USV^T = Co$;
6: $Z_{red} = U \cdot IH(U^\top Z)$.

Assumption 2: The system belongs to the initial model set: $\theta \subset Z(0)$, with $Z(0) = p_0 \bigoplus H_0 B^m$.

The proposed iterative SM identification method to update the zonotope $Z(t+1)$ is described in Algorithm II.

III. Learning Scenario-based Model Predictive Control

The goal of the control strategy is to track a desired output reference and reject disturbances from t=0 up to some finite time step T. Moreover, the controller shall enforce input and output constraints, handling the uncertainty on the model

Algorithm 2 Set Membership Iterative Identification Algorithm

1: Collecting input-output data, obtain $\epsilon_d + \epsilon_v$ and $Z(0)$;
2: For time instant t, build strip
3: $S(t) = \{\theta : |\tilde{y}(l) - \theta^\top z(l)| \leq \epsilon_d + \epsilon_v\}$;
4: Based on $S(t)$, obtain zonotope $Z(t+1)$ by Property 1;
5: Over-estimate zonotope $Z(t+1)$ by reduced order zonotope $Z_{red}(t+1)$ using Algorithm 1.

parameters described by the model set $AFSS(t)$. Therefore, a predictive control strategy is selected.

Let N be the prediction horizon and $u_{k|t}$, $k \in [0, N-1]$, be the candidate future control moves, where the notation $k|t$ indicates the prediction at step $k+t$ given the information at the current step t. The scenario-based MPC proposed in [12] allows to compute an optimal finite-horizon input trajectory $u_{0|t}, ..., u_{N-1|t}$ that is feasible under K sampled scenarios of the uncertainty parametrized by the updated system parameter set $AFSS(t)$.

More concretely, let $\theta(t)^1, ..., \theta(t)^K$ be i.i.d. samples of θ, drawn at time t from $AFSS(t)$, and $\theta(t)^0$ be the center of the zonotope $AFSS(t)$. The adaptive scenario-based MPC problem then reads as follows:

$$\begin{aligned}
\min_{\substack{u_{0|t},\dots,u_{N-1|t},\\ du_{max}}} \quad & \sum_{i=1}^{N} \omega_y (y^0_{i|t} - y_{des}(t+i))^2 + \omega_u u^2_{i|t} + \\
& \omega_c du_{max} \\
\text{s.t.} \quad & y^k_{i|t} = {\theta(t)^k}^\top z^k_{i|t} \\
& z^k_{0|t} = z(t), \forall k = 0, 1, ..., K \\
& |y^k_{i|t}| \leq y_{max} \\
& \forall i = 1, ..., N, k = 0, 1, ..., K \\
& |u_{i|t}| \leq u_{max} \quad \forall i = 0, ..., N-1 \\
& |\Delta u_{i|t}| \leq du_{max} \quad \forall i = 0, ..., N-1, \qquad (7)
\end{aligned}$$

where ω_y, ω_u and ω_c are weighting factors for the tracking error, input signal and soft constraint on $|\Delta u_{i|t}| = |u_{i+1|t} - u_{i|t}|$.

At each time step t, with measured data $y(t)$ and input $u(t-1)$, the model set $Z(t) = p(t) \bigoplus H(t) B^m$ is updated by Property 1 and the set order is reduced by Algorithm 1. Then, $\theta(t)^k$ samples are obtained from the reduced-order zonotope $Z_{red}(t) = p_{red}(t) \bigoplus H_{red}(t) B^m$ as:

$$\theta(t)^k = p_{red}(t) + 2H_{red}(t)(r^k - 0.5) \qquad (8)$$

where r^k is a random vector, whose elements are uniformly distributed in $[0, 1]$.

The sampled models provide K different output trajectories over the prediction horizon, each corresponding to one sequence of affine transition maps defined by a particular scenario $\theta(t)^k$. Note that these K state trajectories are subject to the same input sequence $u_{0|t}, ..., u_{N-1|t}$. The cost function approximates the average behavior of the model set, by considering the model defined by the center of the zonotope. The output constraints are required to hold for all the K sampled state trajectories over the prediction horizon. Once problem (7) is solved, the current input $u(t) = u_{0|t}$ is the first element of the optimal solution $u_{0|t}$,...,$u_{N-1|t}$. The steps for the efficient learning scenario-based MPC strategy are summarized in Algorithm 3.

The scenario number K must be selected carefully to guarantee the desired risk level in the stochastic optimization solution. Lemma 1 from [12] is exploited to determine K by constraining the expectation of output constraint violation probability $E(V_t|y_t)$.

Lemma 1: The following inequality holds [12]: $E(V_t|y_t) \leq \frac{m}{K+1}$.

Algorithm 3 Adaptive Scenario-based MPC Algorithm

1: At time step t, obtain from the system the current measured plant outputs and update the model set based on the new information;
2: Extract K scenarios form the updated model set;
3: Calculate a sequence of possible future control inputs by solving the finite horizon optimal control problem minimizing a weighted quadratic cost involving the tracking error and enforcing the input and output constraints for all K scenarios;
4: Apply the first element of calculated input sequence, set t=t+1, go to 1.

IV. Vehicle Path Following through Learning MPC

The effectiveness of the proposed method is verified through simulations on a path-following control problem for a vehicle, as illustrated in Fig. 1. The system under evaluation combines the bicycle model with an offset dynamic model to capture the vehicle's motion and dynamics, as described in [21]. The resulting compact model is a fourth order linear parameter invariant system expressed in the following form,

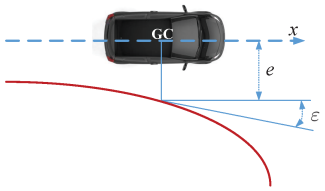

Fig. 1. Vehicle Lateral Offset Dynamic Model Scheme.

$$\begin{bmatrix} \dot{v}_y \\ \dot{r} \\ \dot{e} \\ \dot{\varepsilon} \end{bmatrix} = \begin{bmatrix} -\frac{c_f + c_r}{m v_x} & -v_x + \frac{c_r l_r - c_f l_f}{m v_x} & 0 & 0 \\ \frac{c_r l_r - c_f l_f}{I_z v_x} & -\frac{c_f {l_f}^2 + c_r {l_r}^2}{I_z v_x} & 0 & 0 \\ -1 & 0 & 0 & v_x \\ 0 & -1 & 0 & 0 \end{bmatrix} \begin{bmatrix} v_y \\ r \\ e \\ \varepsilon \end{bmatrix} + \begin{bmatrix} \frac{c_f}{m} \\ \frac{c_f l_f}{I_z} \\ 0 \\ 0 \end{bmatrix} \delta_f + \begin{bmatrix} 0 \\ 0 \\ 0 \\ v_x \end{bmatrix} K_L \qquad (9)$$

where the state variables are v_y lateral speed, r yaw rate, e lateral error and ε heading error. The model parameters are c_f and c_r the cornering stiffness of front and rear tires, m total mass of the vehicle, v_x longitudinal speed, l_f and l_r distances from the front and rear axles to the Gravity Center

(GC) and I_z yaw inertia around the GC. The manipulated input is δ_f the front wheel steering angle, while K_L the curvature of the target road is an input disturbance.

A moving horizon problem in the form (7) is formulated to track a path, while minimizing the lateral offset. The system dynamics are parametrized as in (1), with $y(t) = e(t\Delta T)$, $u(t) = \delta_f(t\Delta T)$, sampled at a rate $\Delta T = 0.1$s. Although system (9) cannot be transformed into the autoregressive form in (1), The disturbance $d(t)$ acting as a UBB input allows for an approximate representation of the system dynamics. To parametrize the model $n_a = 3$ and $n_b = 2$ are employed. The output constraint violation probability is set to $E(V_t|y_t) = 5\%$, requiring $K = 19$ scenarios for the optimization problem (7).

The weights ω_y, ω_u and ω_c are tuned iteratively, while the hard constraint on the input is set as u_{max}=100deg. While a prediction horizon $N = 20$ is chosen to balance computational complexity and control performance.

The simulation environment was implemented in MATLAB, using the Cora toolbox and Yalmip as modeling language, as shown in Fig. 2. The vehicle parameters are listed in Table I. The learning scenario-based MPC with measured data from the vehicle dynamic model is executed in each step as a quadratic programming problem. The optimal steering wheel angle is applied to the continuous-time system model (9), and the model is integrated using a variable step solver. The AFSS is parametrized as a zonotope with $m = 6$ generators, updated as described in Section II, leveraging the CORA toolbox.

TABLE I

MAIN PARAMETERS FOR VEHICLE MODEL

Parameters	Value
m(kg)	1416
I_z(kg· m^2)	3195
l_f(m)	1.0434
l_r(m)	1.5436
C_f(N/rad)	52043
C_r(N/rad)	197970

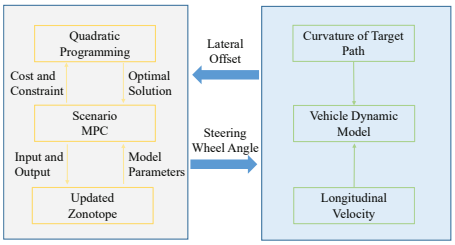

Fig. 2. Simulation in MATLAB.

The initial zonotope $Z(0)$ is obtained by simulating the vehicle dynamic model in open-loop on a double lane change path. The longitudinal velocity is kept constant at 30km/h during data collection.

The control strategy is applied to the vehicle on two different paths. For each path, tests with different measurement noise levels are performed. A test with high measurement noise, $\epsilon_v = 0.1$m and one with low measurement noise, $\epsilon_v = 0.01$m.

The behavior of the manipulated input δ_f and the controlled output e, obtained with the proposed method, are compared with two benchmark methods, which include a robust PID controller from [21] and an adaptive MPC from [17]. The uncertainty set in the second strategy is combined with the iterative SM identification proposed in this work to get a fair comparison.

Case 1: The double lane change maneuver holds significant importance in automotive testing. It is a dynamic driving scenario that simulates a common yet challenging situation encountered by drivers on the road, where a vehicle needs to swiftly and safely change lanes twice in succession, often to avoid an obstacle, merge into traffic, or overtake. This test scenario is crucial for evaluating various aspects of a vehicle's performance, safety, and handling capabilities. Therefore, we use Double Lane Change path as the target path. In Fig. 3 are plotted the trajectory and curvature K_L of the maneuver. Fig. 4 and Fig. 5 depict the steering wheel angle and the lateral offset resulting from the proposed and benchmark methods for a test with measurement noise bound $\epsilon_v = 0.01$m.

It can be noticed that the proposed method is stable and performs a robust regulation of the lateral offset. The performance is close to that of the adaptive MPC. However, the robust MPC for [17] requires solving a more complex optimization problem at each time step. In fact, the original adaptive MPC would enforce constraint satisfaction for all the plants inside the model set, leading to significantly higher computational complexity, where the number of constraints grows with the number of active constraints and the number of outputs, making it computationally expensive for large uncertainty scenarios. In this case study it was required to enlarge the constraints to avoid infeasibility and to limit the considered active constraints from the uncertainty set to handle computational requirements. Meanwhile, in our method the number of constraints is determined by the risk level that remains fixed over time, giving a trade-off between complexity and constraint violation, reducing the computational load, and making the approach more scalable.

In Fig. 6 the volume of the updated zonotope is depicted for the tests with noise 0.1m. The initial reduction of zonotope volume shows that the model rapidly adapts, learning the system dynamics through the SM method. Finally, for quantitative analysis, we list the mean squared error (MSE) and maximum amplitude (MAX) of lateral offset and steering wheel angle of the considered methods in Tables II and III. The data validates the effectiveness of the proposed method.

Case 2: The target path in Case 2 is a complex road course. The path captures a variety of driving scenarios representative of real-world driving. In Fig. 7, the trajectory and curvature of the Road Course are plotted, highlighting the road's varying and complex curvature. Fig. 8 illustrates the steering wheel angle for the test with low noise, showing that the PID controller lacks robustness to noise, while the

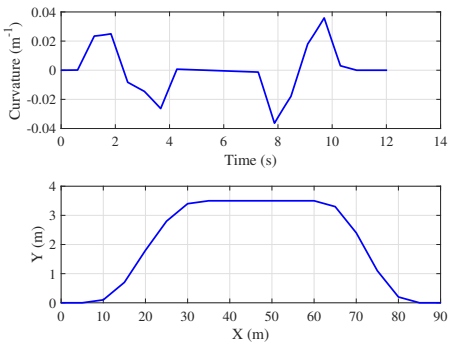

Fig. 3. Curvature and Trajectory of the Double Lane Change Test.

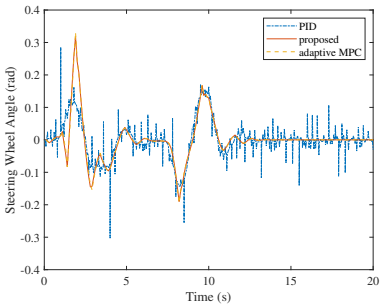

Fig. 4. Steering Wheel Angle Comparison on Double Lane Change Path with Noise 0.01m.

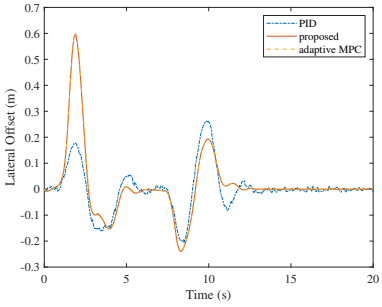

Fig. 5. Lateral Offset Comparison on Double Lane Change Path with Noise 0.01m.

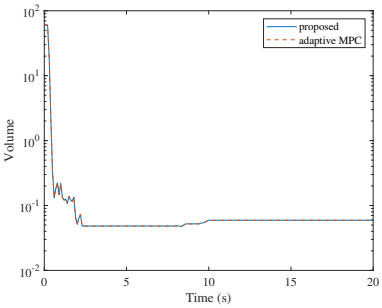

Fig. 6. Zonotope Volume on Double Lane Change Path with Noise 0.1m.

baseline adaptive MPC and the proposed controller provide satisfactory behavior. Fig. 9 presents the lateral offset. The results indicate that the proposed method exhibits performances similar to the adaptive MPC. However, our method is computationally less demanding. The evolution of the zonotope volume is depicted in Fig. 10, while Tables IV and V summarize the results, showing that the RME of lateral offset for the proposed method is the lowest.

TABLE II

PERFORMANCE COMPARISON IN CASE 1 WITH NOISE 0.1M

Methods	Lateral offset		Steering wheel angle	
	MSE	MAX	MSE	MAX $\lvert\Delta u\rvert$
Proposed	0.0076	0.2938	0.0033	0.1410
Adaptive MPC	0.0077	0.2942	0.0033	0.1410
PID	0.0116	0.3393	0.0291	2.0902

TABLE III

PERFORMANCE COMPARISON IN CASE 1 WITH NOISE 0.01M

Methods	Lateral offset		Steering wheel angle	
	MSE	MAX	MSE	MAX $\lvert\Delta u\rvert$
Proposed	0.0164	0.5966	0.0040	0.0875
Adaptive MPC	0.0166	0.6002	0.0040	0.890
PID	0.0069	0.2624	0.0034	0.2662

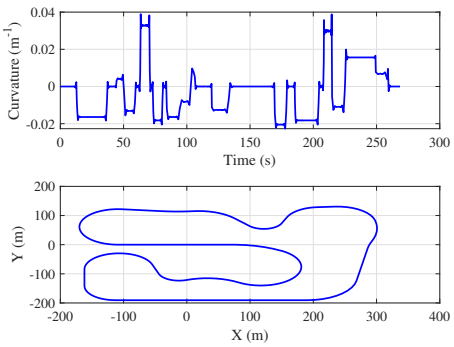

Fig. 7. Curvature and Trajectory of Road Course Test.

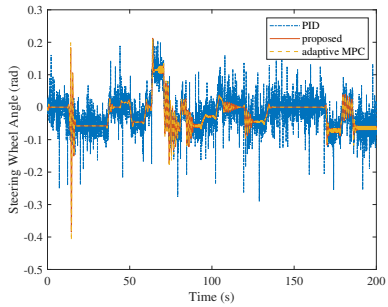

Fig. 8. Steering Wheel Angle Comparison on Road Course Path with Noise 0.01m.

V. CONCLUSIONS

In this research, we have proposed a learning predictive control method with low computational complexity, based

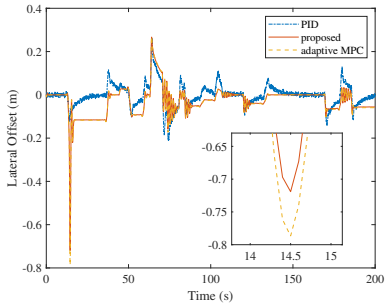

Fig. 9. Lateral Offset Comparison on Road Course Path with Noise 0.01m.

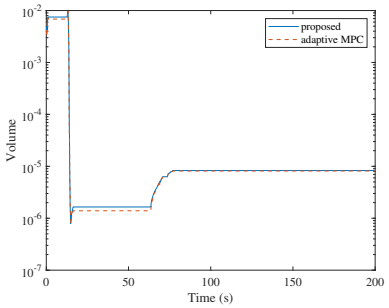

Fig. 10. Zonotope Volume on Road Course Path with Noise 0.01m.

TABLE IV

PERFORMANCE COMPARISON IN CASE 2 WITH NOISE 0.1M

Methods	Lateral offset		Steering wheel angle	
	MSE	MAX	MSE	MAX $\lvert\Delta u\rvert$
Proposed	0.0044	0.2903	0.0029	0.1410
Adaptive MPC	0.0045	0.3613	0.0029	0.1410
PID	0.0067	0.3188	0.0265	2.9052

TABLE V

PERFORMANCE COMPARISON IN CASE 2 WITH NOISE 0.01M

Methods	Lateral offset		Steering wheel angle	
	MSE	MAX	MSE	MAX $\lvert\Delta u\rvert$
Proposed	0.0054	0.65191	0.0025	0.1523
Adaptive MPC	0.0059	0.65868	0.0025	0.1675
PID	0.0026	0.2594	0.0027	0.2662

on scenario-based MPC and Set Membership estimation. An ARX structure is employed to model the system dynamics, while the uncertainty is parametrized using a zonotopic representation. A scenario-based MPC method is combined with the Set Membership identified model to handle uncertainty. An efficient iterative procedure is proposed to update the uncertainty zonotope as new input and output data are acquired at each step, while the zonotopic formulation allows to easily generate scenarios for the randomized optimization problem resulting from the scenario MPC problem. The effectiveness of the proposed MPC is validated through simulations on a vehicle path following problem and compared with two benchmark methods. Future research is focused on extending the model learning setting to time-varying systems.

REFERENCES

[1] D. Q. Mayne. Model predictive control: Recent developments and future promise. *Automatica*, 50(12):2967–2986, 2014.

[2] A. Sasfi, M. N. Zeilinger, and J. Kohler. Robust adaptive MPC using control contraction metrics. *Automatica*, 155:111169, 2023.

[3] S. Chen, V. M. Preciado, M. Morari, and N. Matni. Robust model predictive control with polytopic model uncertainty through system level synthesis. *Automatica*, 162:111431, 2024.

[4] M. E. Villanueva, M. A. Muller, and B. Houska. Configuration-constrained tube MPC. *Automatica*, 163:111543, 2024.

[5] K. I. Kouramas, C. Panos, N. P. Faisca, and E.N. Pistikopoulos. An algorithm for robust explicit/multi-parametric model predictive control. *Automatica*, 49(2):381–389, 2013.

[6] P. Sauerteig, W. Esterhuizen, M. Wilson, T. K. S. Ritschel, K. Worthmann, and S. Streif. Model predictive control tailored to epidemic models. In *2022 European Control Conference (ECC)*, pages 743–748, 2022.

[7] S. Yu, X. Pan, A. Georgiou, B. L. Chen, I. M. Jaimoukha, and S. A. Evangelou. Robust model predictive control framework for energy-optimal adaptive cruise control of battery electric vehicles. In *2022 European Control Conference (ECC)*, pages 1728–1733, 2022.

[8] B. Kouvaritakis, J.A. Rossiter, and J. Schuurmans. Efficient robust predictive control. *IEEE Transactions on Automatic Control*, 45(8):1545–1549, 2000.

[9] D. Q. Mayne, J. B. Rawlings, C. V. Rao, and P. O. M. Scokaert. Constrained model predictive control: Stability and optimality. *Automatica*, 36(6):789–814, 2000.

[10] M. Cannon, B. Kouvaritakis, S. V. Rakovic, and Q. Cheng. Stochastic tubes in model predictive control with probabilistic constraints. *IEEE Transactions on Automatic Control*, 56(1):194–200, 2011.

[11] B. Li, T. Guan, L. Dai, and G. Duan. Distributionally robust model predictive control with output feedback. *IEEE Transactions on Automatic Control*, 69(5):3270–3277, 2024.

[12] G. Schildbach, L. Fagiano, C. Frei, and M. Morari. The scenario approach for stochastic model predictive control with bounds on closed-loop constraint violations. *Automatica*, 50(12):3009–3018, 2014.

[13] F. Micheli and J. Lygeros. Scenario-based stochastic MPC for systems with uncertain dynamics. In *2022 European Control Conference (ECC)*, pages 833–738, 2022.

[14] L. Hewing, K. P. Wabersich, M. Menner, and M. N. Zeilinger. Learning-based model predictive control: Toward safe learning in control. *Annual Review of Control, Robotics, and Autonomous Systems*, 3:269–296, 2020.

[15] T. Alamo, J. M. Bravo, and E. F. Camacho. Guaranteed state estimation by zonotopes. *Automatica*, 41(6):1035–1043, 2005.

[16] M. Milanese and C. Novara. Unified set membership theory for identification, prediction and filtering of nonlinear systems. *Automatica*, 47(10):2141–2151, 2011.

[17] M. Tanaskovic, L. Fagiano, R. Smith, and M. Morari. Adaptive receding horizon control for constrained MIMO systems. *Automatica*, 50(12):3019–3029, 2014.

[18] A. Cordoba-Pacheco, L. Petrucci, M. Filippone, and F. Ruiz. Experimental data-driven bess controller tuning: A set-membership approach. In *2024 IEEE Conference on Control Technology and Applications (CCTA)*, pages 408–413, 2024.

[19] T. Alamo, J. M. Bravo, and E. F. Camacho. Guaranteed state estimation by zonotopes. In *42nd IEEE International Conference on Decision and Control*, pages 5831–5836, 2003.

[20] A. K. Kopetzki, B. Schurmann, and M. Althoff. Methods for order reduction of zonotopes. In *2017 IEEE 56th Annual Conference on Decision and Control (CDC)*, pages 5626–5633, 2017.

[21] Q. Shi and H. Zhang. Road-curvature-range-dependent path following controller design for autonomous ground vehicles subject to stochastic delays. *IEEE Transactions on Intelligent Transportation Systems*, 23(10):17440–17450, 2022.